Homogeneous Electrocatalysis

International Edition: DOI: 10.1002/anie.201904075
German Edition: DOI: 10.1002/ange.201904075

Fast Oxygen Reduction Catalyzed by a Copper(II) Tris(2-pyridylmethyl)amine Complex through a Stepwise Mechanism

*Michiel Langerman and Dennis G. H. Hetterscheid**

Abstract: *Catalytic pathways for the reduction of dioxygen can either lead to the formation of water or peroxide as the reaction product. We demonstrate that the electrocatalytic reduction of O_2 by the pyridylalkylamine copper complex $[Cu(tmpa)(L)]^{2+}$ in a neutral aqueous solution follows a stepwise $4e^-/4H^+$ pathway, in which H_2O_2 is formed as a detectable intermediate and subsequently reduced to H_2O in two separate catalytic reactions. These homogeneous catalytic reactions are shown to be first order in catalyst. Coordination of O_2 to Cu^I was found to be the rate-determining step in the formation of the peroxide intermediate. Furthermore, electrochemical studies of the reaction kinetics revealed a high turnover frequency of $1.5 \times 10^5\ s^{-1}$, the highest reported for any molecular copper catalyst.*

With the shift in the energy landscape from fossil fuels towards sustainable sources of energy, storage and conversion of fuels, such as hydrogen, is expected to play an important role. It is therefore important that efficient fuel cells are available to minimize energy loss during fuel-to-energy interconversion. However, the cathodic oxygen reduction reaction (ORR) is a significant limiting factor in the efficiency of fuel cells.[1] In nature, multicopper oxidases, such as laccase, are known to catalyze the four-electron reduction of O_2 to H_2O efficiently.[2] Immobilization of laccase on electrodes has shown that the ORR can be performed close to the thermodynamic equilibrium potential of water.[3] In an effort to create synthetic mimics of these copper enzymes, a wide range of model copper systems have been studied for their oxygen activation reactivity.[4] While some early examples of copper complexes have been studied for their activity towards the ORR,[5] only in the last decade have the first molecular copper model catalysts been evaluated for their ORR activity, either by means of sacrificial reductants or in electrochemical studies.[6] $[Cu(tmpa)(L)]^{2+}$ (tmpa = tris(2-pyridylmethyl)amine, L = solvent), as well as many derivatives of the pyridylalkylamine template, has been studied as a mimic for active sites in redox-active metalloenzymes for its nonplanar and flexible coordination sphere and its reactivity towards dioxygen.[4e,7] The dioxygen binding chemistry of Cu–tmpa has been thoroughly studied by Karlin and co-workers.[8] It was shown that in a range of solvents, the binding of dioxygen to $[Cu^I(tmpa)]^+$ leads to fast formation of an end-on Cu^{II} superoxo complex, followed by a slower dimerization step to form a dinuclear copper peroxo complex. Additionally, Fukuzumi, Karlin, and co-workers have studied the ORR activity of Cu–tmpa in acetone, using decamethylferrocene as a sacrificial reductant; this reaction involves a dinuclear intermediate.[6a,d] It was shown that Cu–tmpa and several derivatives, adsorbed on carbon black, catalyze the electrochemical ORR in aqueous buffer solutions.[9] The ORR activity of Cu–tmpa in solution has also been investigated, as well as pH effects on the redox chemistry.[10] However, thus far catalytic rates have not been reported, and the mechanism wherein ORR occurs has not been solved.

The field of homogeneous electrocatalysis for the conversion of small molecules (O_2, CO_2, H_2O, H_2, etc.) is expanding rapidly, and great strides have been made to develop new methods to be able to study their reaction kinetics and to allow for benchmarking of different catalysts.[11] Foot-of-the-wave analysis (FOWA) has become an important tool to determine the catalytic performance of homogeneous electrocatalysts, as it allows for the determination of rate constants under limiting conditions.[11a,d,12] Using these methods, we have quantified the fast electrocatalytic ORR by homogeneous Cu–tmpa in neutral aqueous solution. Additionally, a comprehensive study of the product formation using R(R)DE techniques has provided important new insight into the electrocatalytic ORR mechanism, and shows that catalysis occurs by a stepwise mechanism at a single copper center.

The redox and catalytic behavior of Cu–tmpa in a phosphate buffer (PB) solution at pH 7, containing 100 mM phosphate salts (NaH_2PO_4 and Na_2HPO_4), was investigated. Cyclic voltammograms (CVs) of Cu–tmpa were recorded using a glassy carbon (GC) working electrode ($A = 0.0707\ cm^2$). In the presence of argon (1 atm), a well-defined reversible Cu^I/Cu^{II} redox couple was visible at $E_{1/2} = 0.21$ V versus RHE (Figure 1). In the presence of O_2 (1 atm), a peak-shaped catalytic wave appeared with an onset potential at 0.5 V versus RHE. This peak-shaped catalytic wave is characteristic of substrate depletion, thus demonstrating the fast catalysis by Cu–tmpa. The homogeneity of the catalyst was established by electrochemical quartz crystal microbalance (EQCM) experiments, both under noncatalytic and catalytic conditions (see the Supporting Information).[13]

Determination of the relationship between the catalytic current and the catalyst concentration would provide useful insight into the possible mechanism of the ORR. Owing to the low solubility of O_2 in most solvents, aqueous or otherwise, either very high O_2 pressures or low catalyst concentrations must be used to avoid the O_2 mass-transport limitation. By

[*] M. Langerman, D. G. H. Hetterscheid
Leiden Institute of Chemistry, Leiden University
Gorlaeus Laboratories
P.O Box 9502, 2300 RA Leiden (The Netherlands)
E-mail: d.g.h.hetterscheid@chem.leidenuniv.nl
Supporting information and the ORCID identification number(s) for the author(s) of this article can be found under: https://doi.org/10.1002/anie.201904075.

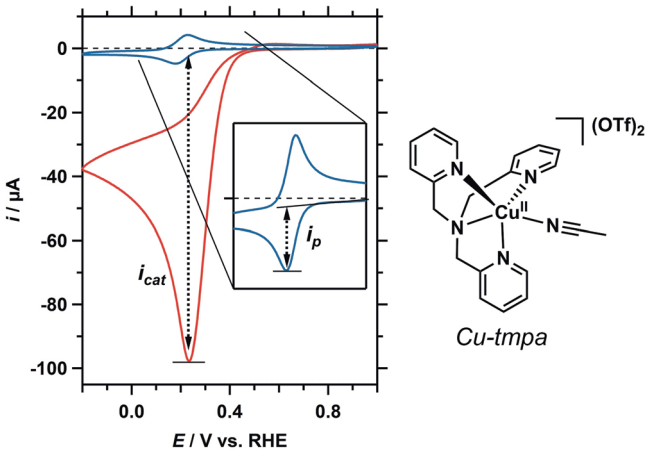

Figure 1. CVs of Cu–tmpa (0.32 mM) in the presence of Ar (1 atm; blue, zoom in inset) or O_2 (1 atm; red). $E_{cat/2} = 0.31$ V versus RHE. Conditions: pH 7 PB ($[PO_4] = 100$ mM), O_2 (1 atm), 293 K, 100 mV s^{-1} scan rate.

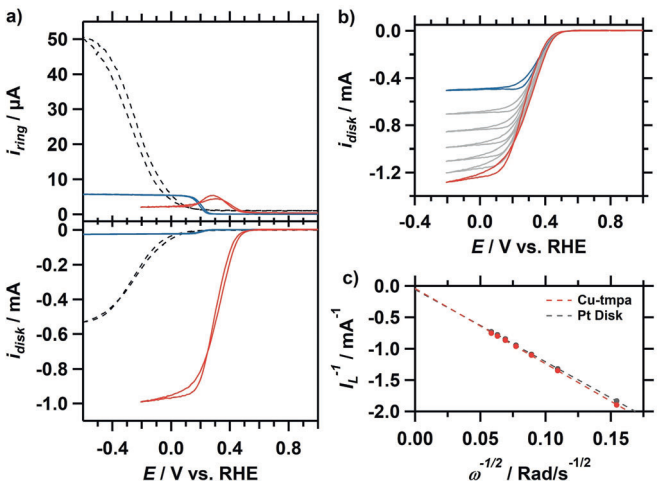

Figure 2. a) RRDE CVs of bare GC (dotted line) under O_2 (1 atm) and Cu–tmpa (0.3 mM) under Ar (1 atm; blue) and O_2 (1 atm; red) at 1600 rpm. b) Disk current of Cu–tmpa (0.3 mM) under O_2 (1 atm) at different rotation rates from 400 rpm (blue line) to 2800 rpm (red line); 400 rpm increments. c) Koutecky–Levich plot of the inverse limiting current (I_L^{-1}) at −0.2 V (vs. RHE) as a function of the inverse square root of the rotation rate. Conditions: pH 7 PB ($[PO_4] = 100$ mM), 293 K, Pt ring at 1.2 V versus RHE, 50 mV s^{-1} scan rate.

measuring CVs in the presence of O_2 (1 atm) at low catalyst concentrations (0.1–1.0 µM Cu–tmpa), a linear first-order dependence of the catalytic current on the catalyst concentration was observed (see Figure S5 in the Supporting Information).

To determine product selectivity and the electron transfer number of the catalyst in neutral aqueous solution, rotating (ring-)disk electrode (R(R)DE) voltammetry was used. Previous hydrodynamic studies on the electrocatalytic ORR performance of Cu–tmpa have been carried out using a Vulcan-supported surface deposit of Cu–tmpa,[9] or only evaluated the behavior of Cu–tmpa in aqueous solution under noncatalytic conditions.[10b] Although R(R)DE voltammetry is most often used to study heterogeneous catalytic reactions, it can be used to study homogeneous catalytic reactions under certain conditions. One of the main difficulties with the use of R(R)DE methods for homogeneous catalysts is that both the product and substrate are present in the liquid phase. For complex multielectron multistep catalytic reactions (ECE or ECEC′), such as the ORR, this can result in significant deviations from the behavior dictated by the Koutecky–Levich (KL) equation, which governs the behavior of reactions with one diffusing species. In such cases, slow catalysis will result in nonideal behavior of the measured limiting currents as a function of the rotation rate, and deviations from linearity will be observed in KL plots. However, for fast catalytic reactions, the limiting current corresponds to the electron transfer number (n) of the catalytic reaction.[14] In effect, sufficiently fast molecular catalysts (where $k \gg$ rotation rate) can be considered to behave as heterogeneous catalysts within this time frame, as is observed in the case of Cu–tmpa. Figure 2A shows a clear positive shift in the ORR onset potential to 0.5 V versus RHE in the presence of Cu–tmpa as compared to the bare GC electrode. KL analysis was performed on the mass-transport limiting current (I_L) obtained at different rotation rates (Figure 2B,C). Indeed, good linearity was observed in the KL plot, similar to that of a Pt disk electrode. This result shows that n is constant as a function of rotation rate under these conditions. The number of electrons involved in the homogeneous ORR catalyzed by Cu–tmpa was determined to be 3.9 (see the Supporting Information), which shows the high selectivity towards the four-electron reduction of dioxygen. This selectivity is in agreement with the heterogenized carbon-black-supported Cu–tmpa system.[9b]

For product determination on the Pt ring electrode, it is important to account for any contributions from reduced catalytic intermediate species towards the observed ring current, as these species could also be oxidized at the ring. A small oxidative ring current can be seen from 0.5 to 0.1 V versus RHE during catalysis, which decreases as the mass-transport-limited current is reached (Figure 2A, red trace). A thorough analysis showed that this behavior can be attributed to H_2O_2 oxidation (see the Supporting Information).

The amount of H_2O_2 produced during ORR as a percentage ($\%H_2O_2$) was quantified using Equation (1) from the disk

$$\%H_2O_2 = \frac{2 \times (i_{ring}/N_{H_2O_2})}{i_{disk} + (i_{ring}/N_{H_2O_2})} \times 100 \quad (1)$$

current (i_{disk}), ring current (i_{ring}), and the collection efficiency of H_2O_2 of the Pt ring ($N_{H_2O_2}$). The $\%H_2O_2$ values were determined from chronoamperometric (CA) measurements at a range of potentials below 0.5 V versus RHE for Cu–tmpa concentrations of 0.3 mM and 1.0 µM (see the Supporting Information). At the onset of the catalytic activity, significant amounts of H_2O_2 were detected, for catalyst concentrations of both 0.3 mM (ca. 75%) and 1.0 µM (ca. 90%; Figure 3). A plateau of $\%H_2O_2$ was clearly visible at the catalytic onset at the lower concentration but less pronounced at the higher catalyst concentration. These percentages decreased with

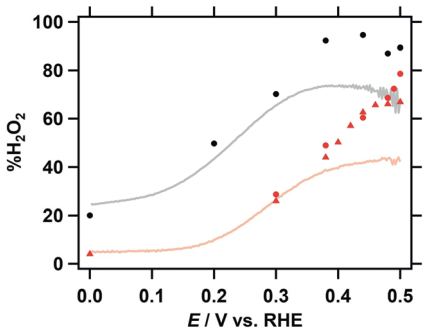

Figure 3. $\%H_2O_2$ obtained from RRDE CA (dots and triangles) and linear sweep voltammetry measurements (lines, 50 $mV s^{-1}$) as a function of applied potential at a rotation rate of 1600 rpm with 0.3 mM (red) and 1.0 μM Cu–tmpa (black). Conditions: pH 7 PB ($[PO_4]$ = 100 mM), 293 K, Pt ring at 1.2 V versus RHE.

decreasing potential, and upon reaching the limiting current potential regime the $\%H_2O_2$ value stabilized at 4 and 20% at 0.0 V versus RHE for 0.3 mM and 1.0 μM Cu–tmpa, respectively. However, below 0.1 V a contribution of the GC electrode towards H_2O_2 production cannot be excluded. These results show that a catalytic reaction that leads to the formation of H_2O_2 is active over the entire catalytic potential window.

Conversion of i_{disk} measured during RDE experiments into the kinetic current density (j_k) enabled the evaluation of Tafel slopes of the ORR in the potential region in which the current was not mass-transport-limited. By plotting the applied potential as a function of the logarithm of j_k, a Tafel plot can be constructed (Figure 4). As we are dealing with

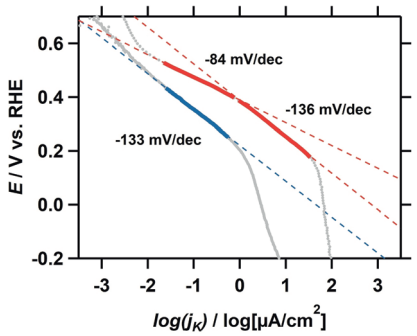

Figure 4. Plot of Tafel slopes derived from RRDE CV at 1600 rpm in the presence of O_2 (1 atm; red lines) or 1.1 mM H_2O_2 (blue line). Conditions: pH 7 PB ($[PO_4]$ = 100 mM), [Cu–tmpa] = 0.3 mM, 293 K, 50 $mV s^{-1}$ scan rate.

a homogeneous multielectron multistep catalytic reaction with several diffusing species, care should be taken not to overinterpret the Tafel slopes or derive specific $e^-/(H^+)$ transfer steps from the Tafel slope values. In the presence of O_2, a clear change in Tafel slope was seen around 0.38 V versus RHE, whereas in the presence of H_2O_2 under otherwise identical conditions no change in slope was observed. The observed slope change during ORR indicates that a different process becomes rate-determining. The potential at which this change occurs closely matches the potential at which half the limiting current is observed and is below the onset potential (ca. 0.45 V) of H_2O_2 reduction by Cu–tmpa (see Figure S14). The Tafel slope observed for the reduction of H_2O_2 by Cu–tmpa is very similar to the $-136\ mV\,dec^{-1}$ slope between 0.38 and 0.20 V during the ORR, which indicates that the same step in the mechanism is rate-determining in this regime. Tafel slopes derived from measurements performed at low (1.0 μM) catalyst concentration showed the same behavior as at higher Cu–tmpa concentration (see Figure S15).

Turnover frequencies (TOFs, s^{-1}) were obtained from electrochemical measurements, either by direct determination using the catalytic current enhancement method,[11b] or by applying foot-of-the-wave analysis (FOWA).[11a,d,12a,b] At the onset of the catalytic wave, the catalytic reaction is assumed to be under kinetic conditions. As such, FOWA is not affected by side phenomena, such as substrate consumption, catalyst deactivation, or product inhibition. It is therefore especially useful for the ORR, in which substrate consumption plays an important role. If more reliable kinetic conditions can be achieved during catalysis, the observed first-order rate constant k_{obs} (or TOF) for the ORR can be directly determined from the catalytic current enhancement (i_{cat}/i_p) by applying Equation (2):

$$\frac{i_{cat}}{i_p} = 2.24n\sqrt{\frac{RT}{Fv}k_{obs}} \qquad (2)$$

in which i_{cat} and i_p refer to the maximum catalytic current and the peak reductive current of the $Cu^{(II/I)}$ redox couple, respectively (Figure 1).[11b] From the current enhancement derived at low catalyst concentration (0.1–1.0 μM), a TOF of $(1.5\times10^5 \pm 0.2\times10^5)\ s^{-1}$ was obtained (see Section 2.10, and Figure S16 in the Supporting Information). This TOF is associated with anoverall 4e catalytic reaction. However, as shown by the RRDE measurements and Tafel slope analysis, there are two different rate-determining catalytic regimes. Interestingly, FOWA can be employed to determine the k_{obs} (or TOF_{max}) associated with the partial reduction of O_2 to H_2O_2, as FOWA only uses the foot of the catalytic wave, where H_2O_2 reduction rates are still negligible. The TOF_{max} for Cu–tmpa in pH 7 phosphate buffer in the presence of O_2 (1 atm) was found to be $(1.8\times10^6 \pm 0.6\times10^6)\ s^{-1}$.

It has been firmly established by stop-flow experiments that oxygen binding to $[Cu^I(tmpa)]^+$ proceeds through a fast equilibrium to initially produce $[Cu^{II}(O_2^{\bullet-})(tmpa)]^+$ as a detectable intermediate.[8b] This species subsequently forms the $[\{Cu^{II}(tmpa)\}_2(\mu\text{-}O_2)]^{2+}$ dimer in a reaction that is consistently slower than the initial oxygen binding over a wide temperature and solvent range. If catalysis were to proceed via such a dimeric species, it should lead to a second-order dependence in Cu–tmpa. Instead, the observed linearity in the FOWA region is in agreement with a catalytic first-order relationship in catalyst (see the Supporting Information),[12a] and is in good agreement with the first-order catalyst-concentration dependence discussed previously. That catalysis can indeed occur at a single-site copper species was demonstrated previously using a site-isolated immobilized

copper phenanthroline system, albeit with a very low catalytic conversion into H_2O_2.[6b]

The TOF_{max} associated with the first $2e^-/2H^+$ reduction step to H_2O_2 is the same, within the error margin, as the TOFs (also determined by FOWA) of the fastest iron porphyrin complexes ($2.2\times10^6\ s^{-1}$) recently reported by Mayer and coworkers, which are the fastest homogeneous ORR catalysts in acetonitrile reported to date.[6e,15] When accounting for the oxygen solubility difference using $TOF = k_{O_2}[O_2]$, where $[O_2] \approx 1.1$ mM in water ($[PO_4] = 100$ mM) under O_2 (1 atm), the obtained second-order rate constant $k_{O_2} = (1.6\times10^9 \pm 0.5\times10^9)\ M^{-1}s^{-1}$ is an order of magnitude faster than those of the aforementioned iron porphyrins. This k_{O_2} is comparable to the second-order rate constant of O_2 binding, $k_{O_2} = 1.3\times10^9\ M^{-1}s^{-1}$, found for Cu^I–tmpa in THF, which represents the fastest k_{O_2} among copper complexes and hemes, both synthetic and natural.[8c]

The $\%H_2O_2$ quantification and analysis of Tafel slopes derived from RRDE measurements provide a strong indication that the ORR proceeds by a stepwise mechanism (Scheme 1). Herein O_2 is first reduced to H_2O_2, which in

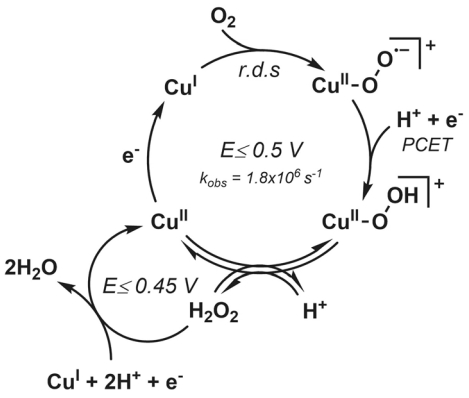

Scheme 1. Proposed stepwise mechanism for the electrocatalytic ORR by Cu–tmpa in neutral aqueous solution. For clarity, the tmpa ligand is not depicted. PCET = proton-coupled electron transfer.

turn is further reduced to H_2O upon reaching the required potential. In this case the overall reaction will still yield a catalytic electron transfer number close to 4 in the O_2 mass-transport-limited regime, as was established by KL and RRDE analysis. The onset potential of H_2O_2 reduction by Cu–tmpa is around 0.45 V versus RHE, roughly 50 mV lower than that of O_2 reduction. The difference between onset potentials is small, which explains why $\%H_2O_2$ quickly decreases when the potential is decreased. At low catalyst concentration a catalyst diffusion effect is observed, and $\%H_2O_2$ is stable over a larger potential range before decreasing. This behavior is expected, as oxygen is a competitive inhibitor for H_2O_2 reduction. Peroxide will accumulate more at low catalyst concentrations, whereas it is more rapidly reduced at higher catalyst loadings while maintaining the same amount of oxygen in solution. As both the ORR Tafel slope below 0.38 V and the Tafel slope for H_2O_2 reduction by Cu–tmpa are the same, it gives a strong indication that the reduction of H_2O_2 to H_2O is rate-determining in this potential window during the ORR. When FOWA is applied to determine the rate constant of the partial reduction of O_2 to H_2O_2, linearity of the catalytic current is only observed when applying the FOWA expression corresponding to a first-order catalytic system (see the Supporting Information). This result shows that the partial reduction of O_2 to H_2O_2 is also first order in catalyst. The initial quantitative accumulation of hydrogen peroxide, the kink in the Tafel slope and its independence of the Cu–tmpa concentration, and the first-order rate dependence on Cu–tmpa point to two separate catalytic cycles, wherein H_2O_2 is readily replaced in the coordination sphere of copper (see Scheme 1).

Our findings contrast with the previously proposed dinuclear mechanism for the ORR by Cu–tmpa using sacrificial reductants in acetone, where fast O_2 binding resulting in a copper superoxo species was followed by a slower dimerization step.[6a] Under aqueous electrochemical conditions, fast electron transfer and high proton mobility allowing for a fast PCET step most likely favor the formation of the hydroperoxo complex over dimerization.

To conclude, the electrocatalytic ORR activity of Cu–tmpa in neutral aqueous solution was quantified, revealing very fast kinetics and high TOFs. The rate constants reported herein are the first rate constants reported for the electrochemical reduction of O_2 by a homogeneous copper complex. Application of FOWA revealed that the TOF associated with the partial reduction of O_2 is very close to the O_2 binding constant with Cu–tmpa. This result suggests that coordination of dioxygen to Cu^I is the rate-determining step in the formation of peroxide. Additionally, we have shown that in aqueous solution the ORR occurs at a single Cu–tmpa center through a stepwise mechanism, in which O_2 first undergoes two-electron reduction to H_2O_2, followed by two-electron reduction of H_2O_2 to H_2O. This stepwise mechanism was first mentioned as one of the possible mechanisms for Cu–tmpa by Asahi et al. on the basis of the ability of Cu–tmpa to catalyze the H_2O_2 reduction.[10a] However, until now there has been no direct evidence that a stepwise reaction takes place during ORR. This study provides new insight into the oxygen reduction reaction mediated by copper, and opens new possibilities for the electrochemical synthesis of hydrogen peroxide that are relevant to energy-conversion reactions, since peroxide is an excellent candidate as a renewable fuel.

Acknowledgements

The European Research Council (ERC) is acknowledged for the funding of this project (ERC starting grant 637556 Cu4Energy to D.G.H.H.).

Conflict of interest

The authors declare no conflict of interest.

Keywords: copper · electrocatalysis · homogeneous catalysis · hydrogen peroxide · oxygen reduction

[1] a) H. A. Gasteiger, S. S. Kocha, B. Sompalli, F. T. Wagner, *Appl. Catal. B* **2005**, *56*, 9 – 35; b) O. Gröger, H. A. Gasteiger, J.-P. Suchsland, *J. Electrochem. Soc.* **2015**, *162*, A2605 – A2622.

[2] E. I. Solomon, U. M. Sundaram, T. E. Machonkin, *Chem. Rev.* **1996**, *96*, 2563 – 2606.

[3] a) V. Soukharev, N. Mano, A. Heller, *J. Am. Chem. Soc.* **2004**, *126*, 8368 – 8369; b) N. Mano, V. Soukharev, A. Heller, *J. Phys. Chem. B* **2006**, *110*, 11180 – 11187; c) C. F. Blanford, R. S. Heath, F. A. Armstrong, *Chem. Commun.* **2007**, 1710 – 1712; d) J. A. Cracknell, K. A. Vincent, F. A. Armstrong, *Chem. Rev.* **2008**, *108*, 2439 – 2461; e) C. F. Blanford, C. E. Foster, R. S. Heath, F. A. Armstrong, *Faraday Discuss.* **2009**, *140*, 319 – 335; f) L. Rulíšek, U. Ryde, *Coord. Chem. Rev.* **2013**, *257*, 445 – 458.

[4] a) E. A. Lewis, W. B. Tolman, *Chem. Rev.* **2004**, *104*, 1047 – 1076; b) J. Serrano-Plana, I. Garcia-Bosch, A. Company, M. Costas, *Acc. Chem. Res.* **2015**, *48*, 2397 – 2406; c) S. Hong, Y.-M. Lee, K. Ray, W. Nam, *Coord. Chem. Rev.* **2017**, *334*, 25 – 42; d) C. E. Elwell, N. L. Gagnon, B. D. Neisen, D. Dhar, A. D. Spaeth, G. M. Yee, W. B. Tolman, *Chem. Rev.* **2017**, *117*, 2059 – 2107; e) L. M. Mirica, X. Ottenwaelder, T. D. P. Stack, *Chem. Rev.* **2004**, *104*, 1013 – 1046.

[5] a) P. Vasudevan, Santosh, N. Mann, S. Tyagi, *Transition Met. Chem.* **1990**, *15*, 81 – 90; b) J. Zhang, F. C. Anson, *J. Electroanal. Chem.* **1992**, *341*, 323 – 341; c) J. Zhang, F. C. Anson, *J. Electroanal. Chem.* **1993**, *348*, 81 – 97; d) J. Zhang, F. C. Anson, *Electrochim. Acta* **1993**, *38*, 2423 – 2429; e) C. C. L. McCrory, X. Ottenwaelder, T. D. P. Stack, C. E. D. Chidsey, *J. Phys. Chem. A* **2007**, *111*, 12641 – 12650.

[6] a) S. Fukuzumi, H. Kotani, H. R. Lucas, K. Doi, T. Suenobu, R. L. Peterson, K. D. Karlin, *J. Am. Chem. Soc.* **2010**, *132*, 6874 – 6875; b) C. C. L. McCrory, A. Devadoss, X. Ottenwaelder, R. D. Lowe, T. D. P. Stack, C. E. D. Chidsey, *J. Am. Chem. Soc.* **2011**, *133*, 3696 – 3699; c) M. A. Thorseth, C. E. Tornow, E. C. M. Tse, A. A. Gewirth, *Coord. Chem. Rev.* **2013**, *257*, 130 – 139; d) S. Kakuda, R. L. Peterson, K. Ohkubo, K. D. Karlin, S. Fukuzumi, *J. Am. Chem. Soc.* **2013**, *135*, 6513 – 6522; e) M. L. Pegis, C. F. Wise, D. J. Martin, J. M. Mayer, *Chem. Rev.* **2018**, *118*, 2340 – 2391; f) S. Fukuzumi, Y.-M. Lee, W. Nam, *ChemCatChem* **2018**, *10*, 9 – 28.

[7] a) K. D. Karlin, J. C. Hayes, S. Juen, J. P. Hutchinson, J. Zubieta, *Inorg. Chem.* **1982**, *21*, 4106 – 4108; b) K. D. Karlin, S. Kaderli, A. D. Zuberbühler, *Acc. Chem. Res.* **1997**, *30*, 139 – 147; c) A. Wada, Y. Honda, S. Yamaguchi, S. Nagatomo, T. Kitagawa, K. Jitsukawa, H. Masuda, *Inorg. Chem.* **2004**, *43*, 5725 – 5735.

[8] a) K. D. Karlin, N. Wei, B. Jung, S. Kaderli, P. Niklaus, A. D. Zuberbuehler, *J. Am. Chem. Soc.* **1993**, *115*, 9506 – 9514; b) C. X. Zhang, S. Kaderli, M. Costas, E.-i. Kim, Y.-M. Neuhold, K. D. Karlin, A. D. Zuberbühler, *Inorg. Chem.* **2003**, *42*, 1807 – 1824; c) H. C. Fry, D. V. Scaltrito, K. D. Karlin, G. J. Meyer, *J. Am. Chem. Soc.* **2003**, *125*, 11866 – 11871.

[9] a) M. A. Thorseth, C. S. Letko, T. B. Rauchfuss, A. A. Gewirth, *Inorg. Chem.* **2011**, *50*, 6158 – 6162; b) M. A. Thorseth, C. S. Letko, E. C. M. Tse, T. B. Rauchfuss, A. A. Gewirth, *Inorg. Chem.* **2013**, *52*, 628 – 634.

[10] a) M. Asahi, S.-i. Yamazaki, S. Itoh, T. Ioroi, *Dalton Trans.* **2014**, *43*, 10705 – 10709; b) M. Asahi, S.-i. Yamazaki, S. Itoh, T. Ioroi, *Electrochim. Acta* **2016**, *211*, 193 – 198.

[11] a) C. Costentin, S. Drouet, M. Robert, J.-M. Savéant, *J. Am. Chem. Soc.* **2012**, *134*, 11235 – 11242; b) R. M. Bullock, A. M. Appel, M. L. Helm, *Chem. Commun.* **2014**, *50*, 3125 – 3143; c) A. M. Appel, M. L. Helm, *ACS Catal.* **2014**, *4*, 630 – 633; d) E. S. Rountree, B. D. McCarthy, T. T. Eisenhart, J. L. Dempsey, *Inorg. Chem.* **2014**, *53*, 9983 – 10002.

[12] a) C. Costentin, J.-M. Savéant, *ChemElectroChem* **2014**, *1*, 1226 – 1236; b) D. J. Wasylenko, C. Rodríguez, M. L. Pegis, J. M. Mayer, *J. Am. Chem. Soc.* **2014**, *136*, 12544 – 12547; c) D. J. Martin, B. D. McCarthy, E. S. Rountree, J. L. Dempsey, *Dalton Trans.* **2016**, *45*, 9970 – 9976; d) C. Costentin, D. G. Nocera, C. N. Brodsky, *Proc. Natl. Acad. Sci. USA* **2017**, *114*, 11303 – 11308; e) C. Costentin, J.-M. Savéant, *J. Am. Chem. Soc.* **2017**, *139*, 8245 – 8250.

[13] a) N. D. Schley, J. D. Blakemore, N. K. Subbaiyan, C. D. Incarvito, F. D'Souza, R. H. Crabtree, G. W. Brudvig, *J. Am. Chem. Soc.* **2011**, *133*, 10473 – 10481; b) D. G. H. Hetterscheid, C. J. M. van der Ham, O. Diaz-Morales, M. W. G. M. Verhoeven, A. Longo, D. Banerjee, J. W. Niemantsverdriet, J. N. H. Reek, M. C. Feiters, *Phys. Chem. Chem. Phys.* **2016**, *18*, 10931 – 10940; c) D. G. H. Hetterscheid, *Chem. Commun.* **2017**, *53*, 10622 – 10631; d) B. van Dijk, J. P. Hofmann, D. G. H. Hetterscheid, *Phys. Chem. Chem. Phys.* **2018**, *20*, 19625 – 19634.

[14] P. A. Malachesky, L. S. Marcoux, R. N. Adams, *J. Phys. Chem.* **1966**, *70*, 4068 – 4070.

[15] M. L. Pegis, B. A. McKeown, N. Kumar, K. Lang, D. J. Wasylenko, X. P. Zhang, S. Raugei, J. M. Mayer, *ACS Cent. Sci.* **2016**, *2*, 850 – 856.

Manuscript received: April 3, 2019
Version of record online: ■■ ■■, ■■■■

Communications

Homogeneous Electrocatalysis

M. Langerman,
D. G. H. Hetterscheid* ——— ▮▮▮▮–▮▮▮▮

Fast Oxygen Reduction Catalyzed by a Copper(II) Tris(2-pyridylmethyl)amine Complex through a Stepwise Mechanism

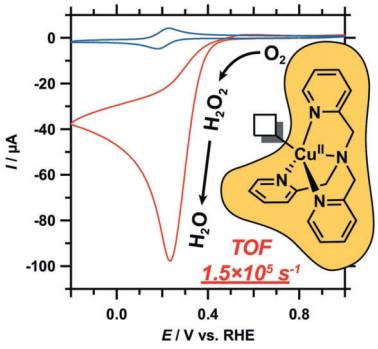

Step by step: The mechanism of the electrochemical reduction of dioxygen by a mononuclear pyridylalkylamine copper complex was investigated (see picture). It was shown that in neutral aqueous solution dioxygen undergoes stepwise reduction, wherein hydrogen peroxide plays a key role. The rate constants determined for this electrocatalytic reaction are among the highest reported for molecular oxygen-reduction catalysts.